Chiral magnetic ordering in two-dimensional ferromagnets with competing Dzyaloshinsky-Moriya interactions

E. Y. Vedmedenko,[1,*] L. Udvardi,[2] P. Weinberger,[3] and R. Wiesendanger[1]
[1]*Institute for Applied Physics, University of Hamburg, Jungiusstrasse 11a, 20355 Hamburg, Germany*
[2]*Department of Theoretical Physics and Center for Applied Mathematics and Computational Physics, Budapest University of Technology and Economics, Budafoki út 8, H -1111, Budapest, Hungary*
[3]*Center for Computational Material Science, Technical University Vienna, Gumpendorfer Strasse 1a, A-1060 Vienna, Austria*
(Received 1 November 2006; revised manuscript received 31 January 2007; published 30 March 2007)

Chiral magnetic ordering due to Dzyaloshinsky-Moriya interaction on two-dimensional lattices is studied theoretically. Several competing Dzyaloshinsky-Moriya vectors are introduced on the basis of symmetry arguments. The role of the exchange interaction, magnetic anisotropy, and dipolar coupling for the ordering in chiral nanomagnets is investigated. It is demonstrated that the periodicity of the modulated structure, which is determined by all interactions involved, is lattice dependent; the direction of spiral propagation and orientation of magnetization is determined by the competition between different Dzyaloshinsky-Moriya vectors and anisotropy; the anisotropy can induce a domain formation or destroy the chiral ordering depending on its orientation. We show that the Dzyaloshinsky-Moriya coupling is responsible for the chiral magnetic ordering in Fe/W(110).

DOI: 10.1103/PhysRevB.75.104431 PACS number(s): 75.30.Et, 75.70.Ak, 75.10.Hk

I. INTRODUCTION

Many magnetic systems possess certain periodicity. The periodicity has at least two length scales—that of an atomic lattice, and that of a magnetic structure. Such structures, which consist of a perfectly periodic crystal, and an additional periodic modulation of some order parameter, are denoted as modulated structures. In centrosymmetric, magnetically ordered crystals the handedness of modulated structures is energetically degenerate. However, if the inversion symmetry is broken for some reasons, this degeneracy may be lifted because the electronic spin-orbit scattering induces chiral asymmetry of exchange coupling.[1] In such noncentrosymmetric systems an additional order parameter—chirality—might appear. The chiral ordering is very interesting from the theoretical point of view as well as for technical applications.

It has been shown recently that antisymmetric exchange interactions first predicted by Dzyaloshinsky[1,2] can be especially strong near magnetic surfaces and in nanostructures due to reduced symmetry and large strains.[3,4] The directions of Dzyaloshinsky-Moriya (DM) vectors have been investigated for several surfaces[4] and the existence of noncollinear magnetic structures in thin films has been postulated. Existing studies of chiral magnetic ordering have been limited up to now to one-dimensional chiral structures with a single DM vector[5] or to frustrated bulk pyrochlores (Ref. 6 and the references therein). The evolution of magnetic nanoordering in mono and/or double layers as a function of length and orientation of several DM vectors has not been investigated so far.

The description of magnetic ordering in two-dimensional systems with several DM vectors is not trivial for several reasons. First, for many lattice symmetries the orientation and the strength of the DM interactions cannot be determined using the theoretical concepts of Ref. 1–4, 7, and 8. Second, different DM couplings may compete, and third, the influence of the magnetic anisotropy on the chiral ordering is not known. Magnetic order on the nanoscale, however, is very important for the description of hysteretic and dynamic properties of nanoobjects.

Though magnetic structuring on the atomic scale is important for an understanding of the physical properties of artificial nanostructures no general theoretical approach has been proposed up to now. The aim of our investigation is to achieve a spatially resolved description of the magnetization patterning in two-dimensional lattices in the presence of competing DM interactions and a magnetocrystalline anisotropy.

II. METHODS

In order to explore the intriguing question as to what extent the competition between several Dzyaloshinsky-Moriya vectors affects the magnetization patterning, we performed Monte Carlo (MC) simulations for samples up to 200×200 classical spins on two-dimensional lattices with open and periodic boundary conditions. Square, rectangular, losenge, and triangular symmetries have been chosen for the calculations as they correspond to different surfaces of sc, bcc, and fcc parent structures for which non-negligible DM interactions have been predicted.[3,4] Additionally we have performed calculations for three-dimensional Fe/W(110) nanowires. However, it has been assumed that the DM interactions have a nonvanishing amplitude only at the surface layer of a nanowire.

The interaction Hamiltonian reads

$$H = J(\vec{R}_{ij})\sum_{i<j}\vec{S}_i\cdot\vec{S}_j + \sum_{i,j}\vec{D}^{\vec{n}}_{\vec{R}_{ij}}\cdot(\vec{S}_i\times\vec{S}_j) + K(\vec{m})\sum_i(\vec{S}_i\cdot\vec{m})^2 + d\sum_{i<j}\left(\frac{\vec{S}_i\cdot\vec{S}_j}{R_{ij}^3} - 3\frac{(\vec{S}_i\cdot\vec{R}_{ij})(\vec{S}_j\cdot\vec{R}_{ij})}{R_{ij}^5}\right), \quad (1)$$

where $\vec{S}_i$ is a three-dimensional unit spin vector at a site i;

 ©2007 The American Physical Society

$\vec{R}_{ij}=\vec{R}_i-\vec{R}_j$ the distance vector between the ith and the jth site and the set $\{\vec{R}_i\}$ defines a three-dimensional lattice $L^{(3)}$. $J(\vec{R}_{ij})$ (negative for ferromagnetic systems) and d denote the strength of the exchange and the dipolar interaction, respectively. The vectorial DM interaction $\vec{D}^{\vec{n}}_{\vec{R}_{ij}}$ depends on both the distance vector $\vec{R}_{ij}$ and the orientation $\vec{n}$ of the DM vector in the three-dimensional space $O^{(3)}$. $K(\vec{m})$ (negative for easy-axis systems) is the uniaxial anisotropy per atom along a direction $\vec{m}$. The calculations have been performed for three-dimensional lattices $L^{(3)}=\{(R_{ix},R_{iy},R_{iz})\}=\{(R_{i\parallel},R_{i\perp})\}$ or on their two-dimensional counterparts $L^{(2)}\subset L^{(3)}$. The plane of $L^{(2)}$ structures is defined by $L^{(2)}=\{R_i^{\parallel}\}=\{(R_{ix},R_{iy})\}$, the orthogonal complement to the $L^{(2)}$ plane being given by $\{R_i^{\perp}\}=\{R_{iz}\}$.

The simulations were performed with an algorithm especially designed for long-range systems: the local fields at each site are computed at the beginning of the simulation and are only updated when a spin-flip attempt is accepted.[9] To check the convergence of the Monte Carlo (MC) procedure for systems with DM interactions we have repeated the calculations with local updates only and with combined local and global updates, where all spins are mirrored at a plane with a randomly chosen normal vector.[9] Good convergence has been obtained in both cases. To prevent artificial effects we did not use a cutoff for evaluation of the dipolar coupling.

In contrast to MC schemes for ferromagnetic systems, where only restricted rotations of the magnetic moment are often used,[10] the rotational space was sampled continuously, i.e., a moment can assume any new angle. This is especially important in dipolar and chiral systems as these interactions often favor large angles between neighboring spins. An extremely slow annealing procedure with up to 150 temperature steps has been applied. To avoid metastable states we have performed two different simulations of the same system simultaneously, starting at different seeds for the random number generator to ensure that the samples take different paths to the equilibrium. Only when both samples reached the same stable energy level it has been taken for granted that the system has reached equilibrium.

III. DZYALOSHINSKY-MORIYA VECTORS FOR DIFFERENT LATTICE SYMMETRIES

According to Refs. 1–4, 7, and 8 the orientation and the amplitude of $\vec{D}^{\vec{n}}_{\vec{R}_{ij}}$ are strongly dependent on the lattice symmetry. In nanomagnets and two-dimensional films antisymmetric exchange coupling is expected to be much stronger than in bulk systems.[4,5] The reduced point group symmetry at surfaces leads to a $\vec{R}_{ij}$ dependence of the DM interaction or, in other words, different DM vectors can be found for different crystallographic directions.

In Fig. 1 the orientations of the nonzero DM vectors[4,7] for four lattice types are shown. According to Ref. 1–4, 7, and 8 nonvanishing $\vec{D}^{\vec{n}}_{\vec{R}_{ij}}$ may exist only for atomic bonds which do not have a center of inversion at their midpoint. Such atomic bonds are schematically drawn in Fig. 1 as connections between lattice points. For example, for a bcc(001) surface [see Fig. 1(a)] nonzero DM interactions are possible only along two perpendicular nearest neighboring bonds. These two DM vectors, however, have different orientations: $\vec{n}_1\perp\vec{n}_2$ [see Fig. 1(a)]. Hence, each nonzero DM vector has two characteristics: the direction of the interaction, $\vec{R}_{ij}$, and the orientation $\vec{n}$. The orientation of the unity vector $\vec{n}$ coincides with that of the DM vector. However, we denote all nonvanishing DM vectors by $\vec{D}^{\vec{n}}_{\vec{R}_{ij}}$ in order to provide explicit information on two very important characteristics of the DM interaction.

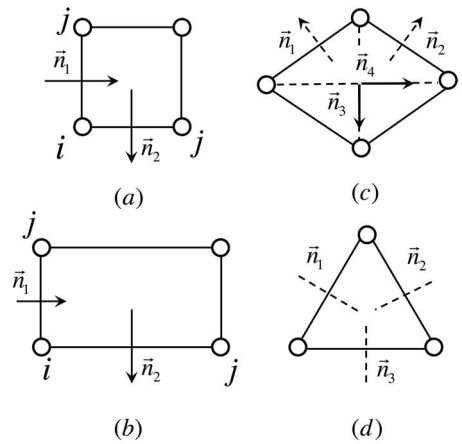

FIG. 1. Orientations $\vec{n}$ of nonzero DM vectors $\vec{D}^{\vec{n}}_{\vec{R}_{ij}}$ for (a) a bcc(001) (square lattice), (b) a sc(110) (rectangular lattice), (c) a bcc(110) (losenge lattice), and (d) an fcc(111) (triangular lattice) surfaces. Panels (a) and (b): the $\vec{n}$ are from the Refs. 1–4, 7, and 8, the moduli of the vectors can be different for different systems. Panel (c): the $\vec{n}$ are lying in the lattice plane but the angle between $\vec{n}$ and $\vec{R}_{ij}$ cannot be determined (Refs. 1–4, 7, and 8). Panel (d): the $\vec{n}$ are in a plane perpendicular to $\vec{R}_{ij}$, but their orientation cannot be determined according to Refs. 1–4, 7, and 8.

While the orientations $\vec{n}$ can be established for the bcc(001) and the sc(110) surface from the theoretical concepts in Ref. 1–4, 7, and 8, for the fcc(111) and the bcc(110) surfaces these orientations are not known. The length of different DM vectors can vary widely for different systems with similar lattice geometry. Therefore, a general description of the magnetic ordering in two-dimensional systems as a function of the modulus and the orientation of the DM vectors is necessary. In the following we explore the magnetic configurational space as a function of the ratio $|\vec{D}^{\vec{n}}_{\vec{R}_{ij}}|/J$ for different surfaces of cubic structures.

IV. RESULTS

A. One nonzero Dzyaloshinsky-Moriya vector

Generally both the DM and the exchange interaction can act between nearest neighbors as well as between more distant sites. For the sake of simplicity we first discuss a simple situation when only one $\vec{D}^{\vec{n}}_{\vec{R}_{ij}}$ vector exists and only a nearest neighbor ferromagnetic exchange interaction J is present. The dipolar interaction and the anisotropy are not considered in this first set of calculations.

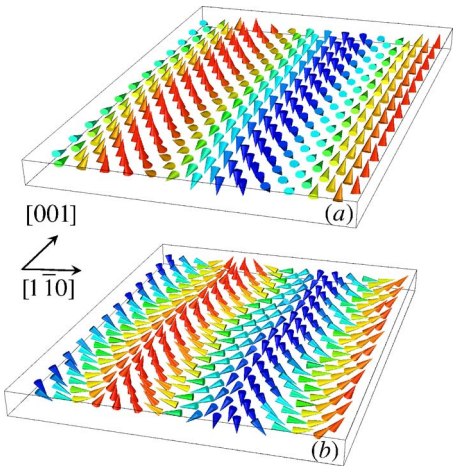

FIG. 2. (Color online) Perspective view of stable Monte Carlo magnetization configurations for a bcc(110) surface at the temperature $kT=0.05J$: (a) $|\vec{D}^{[1\bar{1}0]}_{[1\bar{1}0]}|=0.3J$; (b) $|\vec{D}^{[001]}_{[1\bar{1}0]}|=0.3J$. The three-dimensional magnetic moments are represented as cones. Shades of grey (colors) denote the vertical component of the magnetization. Perpendicular to the plane, the $L^{(2)}$ component of magnetization S_z rotates from +1 (grey/red) to −1 (dark grey/blue) through $S_z=0$ (light grey/green).

The results of our simulations for a losenge lattice corresponding to bcc(110) surface and a triangular lattice corresponding to fcc(111), hcp(0001), sc(111) or bcc(111) structures are illustrated in Figs. 2 and 3, respectively. In Fig. 2 the DM interaction acts along one of the high symmetry crystallographic directions in the film plane; i.e., $\vec{R}_{ij}\|[1\bar{1}0]$ in Fig. 2. This leads to the fact that the magnetization modulates along $[1\bar{1}0]$ axis while in each atomic row running in $[001]\perp[1\bar{1}0]$ all magnetic moments have identical orientation (see Fig. 2). We call the direction for which the modulation of magnetization occurs the direction of propagation of the spiral state. This direction provides no information about the chirality of the spiral or the spatial orientation of

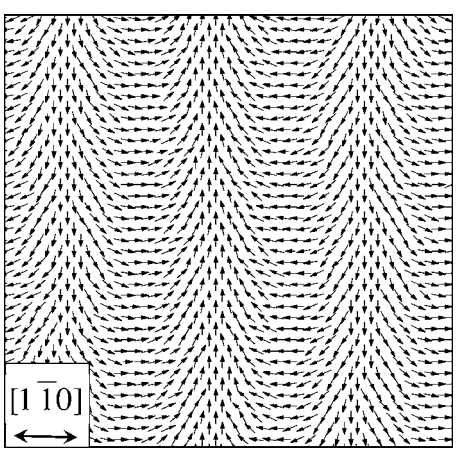

FIG. 3. Top view of a portion of the stable Monte Carlo magnetization configuration on a triangular lattice for $|\vec{D}^{[001]}_{[1\bar{1}0]}|=0.4J$ at $kT/J=0.05$. $\vec{n}$ is perpendicular to the film plane. The magnetic pattern is completely planar.

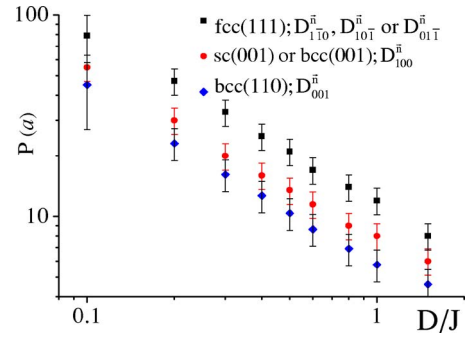

FIG. 4. (Color online) Periodicity of a modulated magnetic structure as a function of $|\vec{D}^{\vec{n}}_{\vec{R}_{ij}}|/J$ for different lattices and directions of propagation.

magnetic moments. These two important features are determined by the orientation $\vec{n}$ of a nonzero DM vector $\vec{D}^{\vec{n}}_{\vec{R}_{ij}}$. In Fig. 2(a) $\vec{R}_{ij}$ is chosen such that $\vec{R}_{ij}\|\vec{n}$ while in Fig. 2(b) $\vec{R}_{ij}\perp\vec{n}$. In other words, in the first case the propagation direction coincides with the orientation of the DM vector whereas in the latter case the two directions are perpendicular. As a result one finds a Bloch-type rotation for $\vec{R}_{ij}\|\vec{n}$ (the rotation occurs in the plane which is perpendicular to the propagation direction), whereas Néel like (the rotation occurs in the plane which is parallel to the propagation direction) for $\vec{R}_{ij}\perp\vec{n}$. As can be expected from the Hamiltonian in Eq. (1) in both cases the rotation plane is perpendicular to the orientation $\vec{n}$ of the DM vector. The chirality is clockwise with respect to $\vec{n}$ for a positive DM term and anticlockwise for a negative one.

An interesting effect has been found for a DM vector parallel to the z axis [001] direction for an fcc(111) symmetry. According to Refs. 4 and 7 such a situation is possible in lattices with a hexagonal symmetry. In Fig. 3 the results of our calculations for $|\vec{D}^{[001]}_{[1\bar{1}0]}|=0.4J$ at low temperature $kT=0.05J$ are shown. As in the previous cases the modulation propagates in the direction $[1\bar{1}0]$ with somewhat larger periodicity. Unlike the previous systems, however, the DM vector is perpendicular to the $L^{(2)}$ plane. Therefore, the rotation is confined to the film plane and a planar, Néel-, wave-like magnetization pattern is formed (see Fig. 3).

Qualitatively the picture is similar for other propagation directions and other lattices. To make this analysis quantitative we define the periodicity of the modulated structure as the number of next nearest distances, na_{nn}, after which identical patterning is achieved. The periodicity P of a magnetization configuration does not depend on the orientation of the DM vector. However, it depends on the lattice symmetry. The periodicity for different lattices are displayed in Fig. 4. P is determined by the competition between the exchange and the DM interaction energy. Hence, P increases with a decreasing ratio $|\vec{D}^{\vec{n}}_{\vec{R}_{ij}}|/J$. The log-log plot (see Fig. 4) reveals a power law $P\propto(|\vec{D}^{\vec{n}}_{\vec{R}_{ij}}|/J)^{-\beta(D/J)}$ for all types of studied lattices. In the region $0.3<|\vec{D}^{\vec{n}}_{\vec{R}_{ij}}|/J<1$ the exponent β is close to 0.8. For $|\vec{D}^{\vec{n}}_{\vec{R}_{ij}}|/J>1.5$, $P\to 2a_{nn}$ and, hence, $\beta\to 0$.

For $|\vec{D}^{\vec{n}}_{\vec{R}_{ij}}|/J<0.1$, β seems to be close to unity, although the accuracy of our calculations in this region is low because of the large periodicity and imperfection of spirals. We believe that the data show a crossover from $\beta=1$ for weak DM interaction to $\beta=0$ at high $|\vec{D}^{\vec{n}}_{\vec{R}_{ij}}|$ values.

For the identical ratios $\vec{D}^{\vec{n}}_{\vec{R}_{ij}}|/J$ the periodicity of lattices with smaller coordination numbers q is smaller. For example, for $D/J=0.2$ P increases from $30a_{nn}$ for a bcc(001) (square lattice) to almost $60a_{nn}$ for a fcc(111) surface (a triangular lattice). This happens because the total exchange energy per spin $E_{\text{exch}}=qJ$, which competes with the DM energy in establishing the periodicity of a spiral, is larger for lattices with higher coordination numbers. Hence, in closer packed systems the exchange coupling is more efficient in competition with the chiral DM interaction.

If the spiral is directed along one of the next nearest neighboring directions P decreases further because of inefficiency of the direct exchange. An example provides a losenge lattice, which corresponds to the (110) surface of a bcc parent lattice. For the spiral propagating in $[1\bar{1}0]$ direction ($\vec{D}^{\vec{n}}_{001}$) we find $P\approx 20a_{nn}$ (see Fig. 4). Thus, for identical $|\vec{D}^{\vec{n}}_{\vec{R}_{ij}}|/J$ ratio the periodicity of the DM spirals propagating along high symmetry directions of a lattice is somewhat larger than those along other directions because of the competition between the DM and the strong exchange interaction.

B. Influence of magnetic anisotropy

Ultrathin magnetic structures very often possess an out-of-plane [like 1–5 ML Co on Au(111), double Fe layer on W(110) or Fe/Au(001)] or an in-plane [like Fe monolayer on W(110) or Co/Cu(001)] crystalline anisotropy.[11] An out-of-plane anisotropy competes with the shape anisotropy arising from the magnetic dipole-dipole interaction. Depending on the orientation an in-plane uniaxial crystalline anisotropy can compete with or stabilize the DM coupling and the dipolar energy. To get a general insight into the influence of the anisotropy on the magnetic structuring in the presence of DM coupling we investigated the magnetic chiral ordering for different ratios $K(\vec{m})/J$ and d/J. In Refs. 4 and 12 the DM vector has been estimated to be of the order of $|\vec{D}^{\vec{n}}_{\vec{R}_{ij}}|/J\approx 0.1$. In ultrathin nanostructures this value can be even larger. Therefore $|\vec{D}^{[1\bar{1}0]}_{[001]}|/J=0.2$ has been used in the calculations. The uniaxial anisotropy has been varied in the interval $0<K(\vec{m})/J<0.2$ as for magnetic nanostructures huge anisotropy values have been reported.[13,14] The dipole-dipole coupling has been varied between $d=0$ and $d=0.01J$ which is reasonable for monolayers of $3d$ metals on metallic substrates.[15]

Figure 5 shows the square of the vertical component of magnetization, S_z, as a function of the anisotropy energy per atom. Interestingly enough the curves $\langle S_z^2\rangle=f(K([1\bar{1}0]))$ and $\langle S_z^2\rangle=f(K([001]))$ are strongly different. For $K([001])$, which is oriented perpendicularly to the DM vector $\vec{D}^{[1\bar{1}0]}_{[001]}$, $\langle S_z^2\rangle$ is nonzero until $K([001])/J\approx|\vec{D}^{[1\bar{1}0]}_{[001]}|/J=0.2$. For $K([1\bar{1}0])$; i.e., for $\vec{m}$ being parallel to the DM vector, $\langle S_z^2\rangle=0$ already for $K([1\bar{1}0])/J\approx 0.05$. The reason for such a behavior can be understood from the magnetic structuring corresponding to each type of anisotropy.

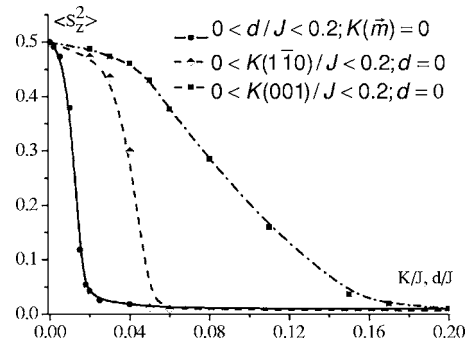

FIG. 5. Plot of $\langle S_z^2\rangle$ versus the anisotropy energy per atom or dipolar constant in units of the exchange constant, where S_z is the component of magnetization perpendicular to the film plane. The magnetic configurations have been obtained for a free-standing monolayer with a bcc(110) stacking; i.e., a losenge lattice, with the DM interaction acting along the [001] direction [$\vec{n}_3$ in Fig. 1(c)]. The results for $K([1\bar{1}0])$ and $K([001])$ are presented; $|\vec{D}^{[1\bar{1}0]}_{[001]}|/J=0.2$; $kT/J=0.01$.

If $K(\vec{m})$ is perpendicular to $\vec{D}^{\vec{n}}_{\vec{R}_{ij}}$ the DM term requires a nonzero projection of magnetization on the $K(\vec{m})$ axis because the magnetization rotates in the plane perpendicular to $\vec{D}^{\vec{n}}_{\vec{R}_{ij}}$. This is the case of $K([001])$ [see Fig. 6(a)]. When $K(\vec{m})\parallel\vec{D}^{\vec{n}}_{\vec{R}_{ij}}$ the DM term requires a zero projection of the magnetization on the direction of anisotropy. This is the case of $K([1\bar{1}0])$. A gain in energy due to a magnetocrystalline anisotropy is associated in the first case $[K(\vec{m})\perp\vec{D}^{\vec{n}}_{\vec{R}_{ij}}]$ by increasing the width of regions with large projections of magnetization on the $K(\vec{m})$ axis. As follows from Fig. 6(a) this disturbs the balance between different orientations lying in the plane of rotation and leads to domain formation. The periodicity of the pattern and the magnetization profile change drastically but the domain structure is very stable. For $K([001])/J=0.03$ we find $\langle S_{001}^2\rangle\approx 0.680\pm 0.003$; $\langle S_z^2\rangle\approx 0.317\pm 0.0028$ and $\langle S_{1\bar{1}0}^2\rangle\approx 0.003\pm 3.5\times 10^{-4}$. Hence, despite the imbalance between different orientations the magnetization remains in the (100) or (xz) plane, which in turn is perpendicular to the DM vector. The very small amount of a $[1\bar{1}0]$ component of magnetization is due to thermal fluctuations ($kT/J\approx 0.01$).

In the case of $K(\vec{m})\parallel\vec{D}^{\vec{n}}_{\vec{R}_{ij}}$ the domain formation does not result in any gain of the anisotropy energy. Therefore the periodicity of the pattern remains the same while the system tries to increase the $y([1\bar{1}0])$ component of the magnetization [see Fig. 6(b)]. For $K([1\bar{1}0])/J=0.03$ we find $\langle S_{001}^2\rangle\approx 0.47\pm 0.02$; $\langle S_z^2\rangle\approx 0.43\pm 0.023$ and $\langle S_{1\bar{1}0}^2\rangle\approx 0.1\pm 0.015$. This large y component [see Fig. 6(b)] cannot be explained

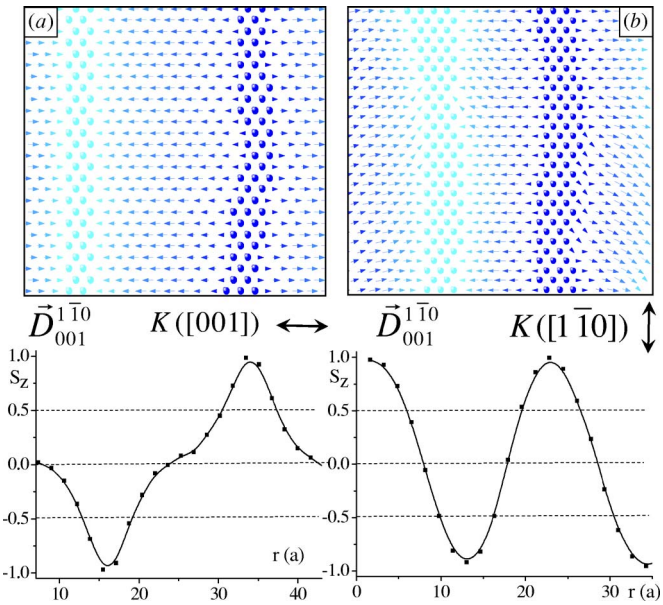

FIG. 6. (Color online) Top view of portions of stable MC configurations and magnetization profiles on a free standing bcc(110) monolayer for (a) $K([001])$ and (b) $K([1\bar{1}0])$. The amplitude of the anisotropy is identical in both cases $K(\vec{m})=0.03J$; $D^{[1\bar{1}0]}_{[001]}$; $kT/J=0.01$. The color scheme denotes the vertical component S_z of the magnetization.

by thermal fluctuations anymore. However, the increase in the magnetization component parallel to the DM vector is incompatible with the DM term. Therefore already very low values of $K(\vec{m})\|\vec{D}^{\vec{n}}_{\vec{R}_{ij}}$ destroy the chiral ordering. The same is true for the dipole-dipole coupling (see Fig. 5). It is known[16] that the dipolar interaction induces a lattice dependent anisotropy; i.e., the magnetic moments try to form chains along principal crystallographic directions of a lattice. When these directions do not coincide with the plane defined by the DM coupling, as in the described case, the dipolar interaction of magnitude $d/J \geqslant 0.05|\vec{D}^{\vec{n}}_{\vec{R}_{ij}}|$ destroys the DM spiral rotation in favor of a vortex formation.

C. Several nonvanishing Dzyaloshinsky-Moriya vectors

In the following we investigate the magnetic ordering in the most common situation when at least two DM vectors are present. As has been shown above each of the DM vectors induces a spiral rotation of periodicity $P \propto (|\vec{D}^{\vec{n}}_{\vec{R}_{ij}}|/J)^{-\beta}$ in the plane perpendicular to the $\vec{D}^{\vec{n}}_{\vec{R}_{ij}}$. Different vectors $\vec{D}^{\vec{n}}_{\vec{R}_{ij}}$ compete for the direction of propagation as well as for the orientation of magnetic moments. First, we explore magnetic ordering as a function of the relative length of two DM vectors for the example of a square lattice. Then, we compare ferromagnetic modulated structures in lattices of different geometry.

Usually, in systems consisting of one sort of atoms the DM vectors make a left- or a right-hand vortex around the site i (see Fig. 2 of Ref. 4). In alloys or nano-objects the situation might be different. For the sake of generality we explore all possible relative orientations of DM vectors. Generally, we find that if several DM vectors exist the magnetic ground state is a superposition of spirals. This superposition is nontrivial as quite a few configurations depending on the phase, strength, and sign of the initial spirals are possible. In addition the lattice symmetry and the strength of the exchange interaction play a very important role. For the calculations on a square lattice we considered two perpendicular DM vectors as shown in Figs. 1(a) and 1(b). One of the vectors propagates along the [100] axis and is oriented parallel to [010] while another one runs along the [010] direction and is of the [100] orientation.

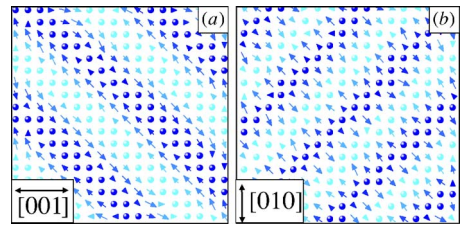

FIG. 7. (Color online) Top view of portions of stable MC configurations for a simple cubic lattice corresponding to a free standing bcc(001) monolayer with a ferromagnetic exchange interaction. (a) $|\vec{D}^{[010]}_{[100]}|=0.8J=-|\vec{D}^{[100]}_{[010]}|$; (b) $|\vec{D}^{[010]}_{[100]}|=0.8J=|\vec{D}^{[100]}_{[010]}|$; $kT/J=0.05$. The insets at the bottom of (a) and (b) give averaged magnetization profiles along [001] direction for the two cases. The color scheme denotes the vertical component of magnetization S_z.

If both DM vectors are of identical length the propagation direction $\vec{R}_p$ of the modulated structure forms an angle of 45 degrees with respect to each axis of high symmetry (see Fig. 7). There are two possibilities for such an orientation: [110] and $[1\bar{1}0]$. The two directions are energetically degenerated. Apparently the same should be true for the orientation of magnetization. For $|\vec{D}^{[010]}_{[100]}|=|\vec{D}^{[100]}_{[010]}|$ the magnetic moments are oriented with an angle of 45° with respect to the principal axes. However, for each direction of propagation characterized by a vector $\vec{R}_p$ two magnetization orientations are possible: parallel or perpendicular to $\vec{R}_p$. Our calculations demonstrate that a sign of the DM interaction plays a crucial role for the orientation of magnetization. The sign of each DM vector determines the chirality of a spiral. For a single DM vector the spirals with opposite chirality have identical energy, but the energy of a superimposed state depends on the chirality of each constituent. While for $|\vec{D}^{[010]}_{[100]}|=|\vec{D}^{[100]}_{[010]}|$ and $\vec{D}^{[010]}_{[100]}\cdot[010]=-\vec{D}^{[100]}_{[010]}\cdot[100]$ a Bloch-like rotation is energetically favorable [see Fig. 7(a)], for $|\vec{D}^{[010]}_{[100]}|=|\vec{D}^{[100]}_{[010]}|$ with $\vec{D}^{[010]}_{[100]}\cdot[010]=\vec{D}^{[100]}_{[010]}\cdot[100]$ the Néel type of rotation applies [see Fig. 7(a)].

The orientation of $\vec{R}_p$ as well as the magnetization orientation depend on the ratio $Q=|\vec{D}^{[001]}_{[010]}|/|\vec{D}^{[010]}_{[001]}|$. This dependence is highly nonlinear. In the bottom panel of Fig. 8 a schematic representation of the modulated structure and the orientation of magnetization for different Q is displayed. To

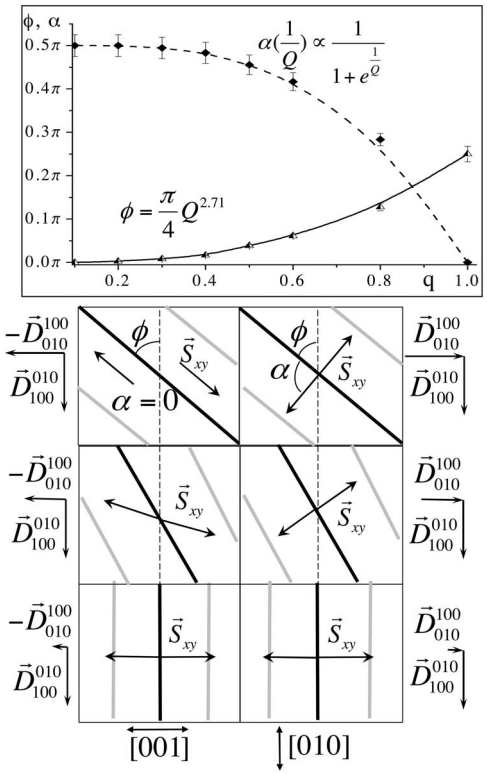

FIG. 8. Top panel: angle ϕ between the direction of uniform magnetization and the [010] axis and angle α between the direction of a uniform magnetization and an in-plane orientation of magnetization $\vec{S}_{xy}$ as a function of the ratio $Q=|\vec{D}^{[010]}_{[100]}|/|\vec{D}^{[100]}_{[010]}|$ for a simple cubic lattice corresponding to a free standing bcc(001) monolayer with a ferromagnetic exchange interaction. Bottom panel: schematic representation of the orientation of the magnetization $\vec{S}_{xy}$ (thick black arrows) with respect to the direction of a uniform magnetization (thick black and white lines) as a function of Q. The moduli and orientations of the DM vectors $\vec{D}^{[010]}_{[100]}$ and $\vec{D}^{[100]}_{[010]}$ are shown explicitly.

characterize quantitatively the two orientations in question we have defined two angles. The angle ϕ is the angle between the [010] axis and the magnetic "domain walls;" i.e., the lines of magnetic moments with identical orientation (thick black and grey lines in Fig. 7, see also Fig. 8). With this definition $\phi+\pi/2$ gives the angle of the propagator $\vec{R}_p$ with respect to the [010] direction. The angle α in Fig. 7 denotes the orientation of the in-plane components of magnetization, $\vec{S}_{xy}$, relative to the direction of domain walls. The moduli and the orientations of the two DM vectors are shown on the left- and right-hand sides of Fig. 8.

As can be seen from the bottom panel of Fig. 8 the angle ϕ does not depend on the sign of the DM term for a square lattice. The function $\phi=f(Q)$ is shown in the top panel of Fig. 8. Within the accuracy of our calculations it follows a power law with the exponent 2.71. The situation with the orientation of magnetization α is more complicated: α always equals $\pi/2$ for opposite senses of rotation of the initial spirals. This means that for any relative strength of two DM interactions of opposite sign the rotation is Néel-like. For both DM vectors being either both positive or both negative

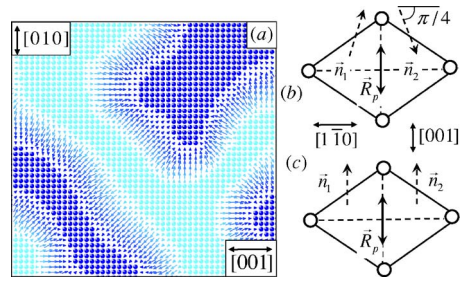

FIG. 9. (Color online) (a) Top view of a portion of a domain wall between energetically degenerated regions of a periodic DM modulation on a square lattice corresponding to a free standing bcc(001) monolayer with a ferromagnetic exchange interaction. The system is characterized by two DM vectors: $|\vec{D}^{[010]}_{[100]}|=|\vec{D}^{[100]}_{[010]}|=0.2J$; (b) and (c) schematic representation of the orientation of DM vectors leading to the perfect chirality of $[1\bar{1}0]$ domain walls in Fe/W(110) with (b) a Néel and (c) a Bloch rotation of magnetization.

the rotation changes from Néel-like to Bloch-like with increasing Q. The $\alpha(Q)$ dependence cannot be described by a power law but shows Boltzmann growth $\alpha(1/Q)\propto\frac{1}{1+1/Q}$.

Because of the energetic degeneration of the two propagation directions on the (100) surfaces we find domain formation in samples with DM interactions. The energy cost for domain walls is small (<2% of the total energy) for realistic values of $|\vec{D}^{\vec{n}}_{\vec{R}_{ij}}|$ as a very smooth transition from one spiral orientation to the other is possible. A typical domain wall generated by the Monte Carlo procedure on a square lattice is shown in Fig. 9(a).

The mechanism of the chiral rotation on other surfaces with several DM vectors is similar to that described above. We always find a superposition of initial spirals. However, if the angle between orientations of the initial DM vectors is different from $\pi/2$ or π the chirality of initial spirals influences both $\phi(Q)$ and $\alpha(Q)$ dependencies. Hence, the direction of propagator $\vec{R}_p$ and the magnetization orientation strongly depend on the magnitude, the orientation, and the chirality of the DM vectors. The functions $\phi(Q)$ and $\alpha(Q)$ vary with respect to the exchange, the DM and the anisotropy parameters; i.e., are material specific. The influence of the on-site anisotropy and the dipolar interaction is similar to that described for spirals occurring for a single $\vec{D}^{\vec{n}}_{\vec{R}_{ij}}$. If an anisotropy axis coincides with an orientation of the magnetization required by the DM coupling the formation of magnetic domains is favored. If the anisotropy is perpendicular to the ideal plane of rotation it destroys the modulation of the magnetic ordering. In order to demonstrate to which complexity of magnetic ordering the competition between different DM vectors can lead we discuss in the following the losenge lattice for the example of Fe/W(110).

D. Chirality of domain walls in Fe/W(110)

Double Fe layers on a stepped W(110) substrate have been extensively studied experimentally and theoretically.[17–21] This very interesting system is character-

ized by alternating monolayer and double layer growth. Both regions show a periodic magnetic domain structure. The periodicity of the pattern as well as the width of mono and/or double layer regions depends on the Fe coverage. The typical distance between adjacent walls for the coverage of 1.7 monolayers is of the order of 20 nm. The domains are separated by 180° domain walls which always run along the $[1\bar{1}0]$ direction. While in monolayers domains with two opposite in-plane orientations have been observed, in double layers out-of-plane domains alternatingly magnetized up and down exist. Experimentally a perfect chirality of magnetic domain walls for the whole area of a large sample has been reported.[18,20] This finding has never been supported by theoretical studies although all other parameters like the orientation of domain walls or the domain size have been described theoretically.[21]

Perfect chirality can appear due to DM interactions predicted to be non-negligible on ultrathin (110) surfaces of cubic crystals.[3,4,12] However, the theoretical concepts in Refs. 3, 4, and 12 cannot predict an exact orientation of the DM vectors as shown in Fig. 1(c). The only statement for a bcc(110) surface made in the Refs. 3, 4, and 12 is that the two vectors should lie in the film plane.

To check whether the uniqueness of the chirality of the domain walls in Fe/W(110) is due to DM interactions we first studied the magnetic structuring for two DM vectors as discussed in Ref. 4 [vectors n_1 and n_2 in Fig. 1(c)]. We repeated the calculations of Ref. 21 using a Hamiltonian with a DM term. As the DM interaction vanishes if there is a center of inversion between cites i and j, it is expected to be relevant only when the local symmetry is sufficiently low. Therefore, nonvanishing DM interactions have been introduced only between cites belonging to the upper plane of the double layer. All other interactions have been applied to the whole system. The parameters of the exchange interaction and anisotropy as well as the magnitude of magnetic moments are known from numerous first principles studies,[22,23] the DM vectors, however, are unknown for that system. Therefore, we explored a phase space for $|\vec{D}^{\vec{n}_1}_{[111]}|=|\vec{D}^{\vec{n}_2}_{[1\bar{1}\bar{1}]}|=0.1,\ldots,0.5J$. It follows from our calculations that there is a manifold of modulated magnetic structures depending on the relative orientation and the modulus of $\vec{n}_1$ and $\vec{n}_2$. However, only some solutions support the experimentally observed magnetic domain structure. Two possibilities are schematically shown in Figs. 9(b) and 9(c). The situation in Fig. 9(b) corresponds to domain walls of Néel type, while that of Fig. 9(c) to the Bloch type. In both cases the walls are running along $[1\bar{1}0]\perp\vec{R}_p$.

In conclusion, we have demonstrated that several surface induced DM vectors can compete for the direction of propagation of the modulated structure as well as for the orientation of magnetization. The strength of the DM interaction competes with the exchange interaction and anisotropy in establishing the periodicity and the orientation of the modulated structure. Depending on its orientation the crystalline anisotropy can promote formation of magnetic domains or destroy the chiral ordering. We have shown that the DM interaction is responsible for the perfect chirality of magnetic domain walls in Fe/W(110). However, our calculations demonstrate also that in real nanosystems in which the exchange interaction is long ranged, several DM constants apply, the anisotropy and the dipolar interactions are much stronger than in bulk, the magnetic phase space is huge. Therefore, to get an insight into the magnetic structuring of nano-objects the DM vectors must be accurately calculated in the framework of relativistic *ab initio* studies.

ACKNOWLEDGMENTS

Financial support from the DFG Grant No. SFB668 and the Austrian Science Ministry Grant No. GZ45.547 is gratefully acknowledged.

*Corresponding author. Electronic address: vedmedenko@physnet.uni-hamburg.de

[1] I. Dzyaloshinsky, Sov. Phys. JETP **5**, 1259 (1957).
[2] I. Dzyaloshinsky, J. Phys. Chem. Solids **4**, 241 (1958).
[3] A. Fert, in *Materials Science Forum*, edited by A. Chamberod and J. Hillairat (Transtech Publications, Aedermannsdorf, 1990), Vol. 59-60, p. 439.
[4] A. Crépieux and C. Lacroix, J. Magn. Magn. Mater. **182**, 341 (1998).
[5] A. N. Bogdanov and U. K. Rößler, Phys. Rev. Lett. **87**, 037203 (2001).
[6] M. Elhajal, B. Canals, R. Sunyer, and C. Lacroix, Phys. Rev. B **71**, 094420 (2005).
[7] T. Moriya, Phys. Rev. Lett. **4**, 228 (1960).
[8] T. Moriya, Phys. Rev. **120**, 91 (1960).
[9] A. Hucht, A. Moschel, and K. D. Usadel, J. Magn. Magn. Mater. **148**, 32 (1995).
[10] U. Nowak, R. W. Chantrell, and E. C. Kennedy, Phys. Rev. Lett. **84**, 163 (2000).
[11] U. Gradmann, *Encyclopedia of Materials: Science and Technology Updates* (Elsevier, Oxford, 2005).
[12] A. Fert and P. M. Levy, Phys. Rev. Lett. **44**, 1538 (1980).
[13] P. Gambardella, S. Rusponi, M. Veronese, S. S. Dhesi, C. Grazioli, A. Dallmeyer, I. Cabria, R. Zeller, P. H. Dederichs, K. Kern *et al.*, Science **600**, 1130 (2003).
[14] Y. Mokrousov, G. Bihlmayer, S. Heinze, and S. Blügel, Phys. Rev. Lett. **96**, 147201 (2006).
[15] M. Bode, E. Y. Vedmedenko, K. von Bergmann, A. Kubetzka, P. Ferriani, S. Heinze, and R. Wiesendanger, Nat. Mater. **5**, 477 (2006).
[16] E. Y. Vedmedenko, A. Ghazali, and J.-C. S. Lévy, Phys. Rev. B **59**, 3329 (1999).
[17] A. Kubetzka, O. Pietzsch, M. Bode, and R. Wiesendanger, Phys. Rev. B **63**, 140407(R) (2001).
[18] A. Kubetzka, M. Bode, O. Pietzsch, and R. Wiesendanger, Phys. Rev. Lett. **88**, 057201 (2002).
[19] M. Bode, S. Heinze, A. Kubetzka, O. Pietzsch, X. Nie, G. Bihlmayer, S. Blügel, and R. Wiesendanger, Phys. Rev. Lett. **89**,

237205 (2002).
[20] A. Kubetzka, Ph.D. thesis, University of Hamburg, 2002.
[21] E. Y. Vedmedenko, A. Kubetzka, K. von Bergmann, O. Pietzsch, M. Bode, J. Kirschner, H. P. Oepen, and R. Wiesendanger, Phys. Rev. Lett. **92**, 077207 (2004).
[22] I. Galanakis, M. Alouani, and H. Dreyssé, Phys. Rev. B **62**, 3923 (2000).
[23] X. Qian and W. Hübner, Phys. Rev. B **60**, 16192 (1999).